Available online at BCREC website: https://bcrec.id

Bulletin of Chemical Reaction Engineering & Catalysis, 17 (4) 2022, 768-777

Research Article

Catalytic Hydrothermal Liquefaction of Sugarcane Bagasse: Effect of Crystallization Time of Fe-MCM-41 and Process Parameters

Gopalakrishnan Govindasamy*, Rohit Sharma, Sunu Subramanian

Department of Chemical Engineering, Energy Cluster, School of Engineering, University of Petroleum & Energy Studies (UPES), Dehradun-248007, India.

Received: 6th September 2022; Revised: 6th November 2022; Accepted: 7th November 2022
Available online: 9th November 2022; Published regularly: December 2022

Abstract

Sugarcane is both food and energy crop providing sugar and energy products. Hydrothermal liquefaction (HTL) is gaining importance for the conversion of sugarcane bagasse to bio-oil, whose yield depends on the deoxygenation activity of the catalyst employed and process parameters. In this study, mesoporous Fe-MCM-41 catalysts were synthesized with crystallization time varied from 12 to 72 h, characterized by X-ray Diffraction (XRD), textural analysis, Scanning Electron Microscope (SEM), Energy Dispersive X-ray (EDX), and evaluated for the HTL of sugarcane bagasse. All the Fe-MCM-41 catalysts gave higher bio-oil yield with lower oxygen content compared to non-catalytic HTL, confirmed their deoxygenation activity. Among them, Fe-MCM-41 synthesized after 24 h of crystallization was found to have the highest crystallinity, and surface area thus gave the highest bio-oil yield of 56.2% containing the least amount of oxygen of 15.3 wt% at 250 °C, initial CO pressure of 45 bar, reaction time of 120 min, Water/Biomass weight ratio of 28, Catalyst/Biomass weight ratio of 0.4 and 0.2, respectively. Overall process of HTL of sugarcane bagasse was found to involve two consecutive equilibria, first conversion of lignocellulose of sugarcane bagasse by hydrolysis to water soluble organics (WSO) followed by its deoxygenation to bio-oil.

Keywords: Sugarcane bagasse; Hydrothermal Liquefaction; Bio-oil; MCM-41; Thermochemical Conversion

How to Cite: G. Govindasamy, R. Sharma, S. Subramanian (2022). Catalytic Hydrothermal Liquefaction of Sugarcane Bagasse: Effect of Crystallization Time of Fe-MCM-41 and Process Parameters. *Bulletin of Chemical Reaction Engineering & Catalysis*, 17(4), 768-777 (doi: 10.9767/bcrec.17.4.15781.768-777)

Permalink/DOI: https://doi.org/10.9767/bcrec.17.4.15781.768-777

1. Introduction

Population explosion and increase in per capita consumption led to industrial growth accompanied by a steep increase in consumption of fossil fuels resulting in their fast depletion and increased CO_2 emission [1]. To address this twin issues of energy security and mitigation of global warming, energy transition from fossil to renewable energy is the urgent need [2]. Biofuels are renewable being produced from biomass and also carbon neutral from life cycle view point [3]. Biofuels is the ideal substitute for transportation fuels [4] and a potential feedstock for the production of chemicals [5]. Hence there is a huge research interest for the development of biochemical and thermochemical processes for its production from biomass especially lignocellulose, the most abundant non-edible biomass [6,7]. Sugar industries process the sugarcane into 10-15 wt% sugar, 27-28 wt% sugarcane bagasse (a lignocellulose solid residue) and 4.5-5 wt% molasses (a liquid product rich in sucrose) on dry basis [8]. Sugarcane provides unique flexibility in converting its edible sugar extracted into cane juice, directly in to energy product such as ethanol, practiced in many of the sugar-

* Corresponding Author.
Email: gopalakrishnan@upes.ac.in (G. Govindasamy);
Telp: +91-135-2776053, Fax: +91-135-2776090

cane processing industries in Brazil [9]. As bagasse and molasses are sources of energy or energy products, sugarcane is regarded both as food crop and energy crop, produced to the extent of 1.89 billion tons per annum globally as per United Nations Food and Agriculture Organization in 2020 [10]. Bagasse is mainly utilized as in-house fuel for ethanol distillation and electricity generation [10]. Second important utilization reported is the production of second generation ethanol by biochemical process which involved its pre-treatment to separate out lignin which constituted 20-30 wt% [8]. This necessitated the finding of alternative means for lignin utilization. Further the pretreatment methods led to the formation of inhibitors which interfered with the subsequent fermentation step and increased the operating cost. Among thermochemical processes, hydrothermal liquefaction (HTL) became attractive as it can handle wet biomass thus no need of energy intensive drying step unlike pyrolysis and hydropyrolysis [11]. Energy recovered by the HTL of sugarcane bagasse was reportedly 170% more than energy realized by its direct burning owing to its high moisture content [12]. Ramirez *et al.* compared various thermochemical options of energy production and concluded that energy recovery per kg of sugarcane bagasse was the highest for HTL followed by pyrolysis and then gasification [13]. HTL of lignocellulose biomass mimics the natural geological process of petroleum formation [14] but taking only minutes to hours. HTL is carried out with hot compressed water which depolymerizes the biopolymers, such as hemicellulose, cellulose and lignin, by hydrolysis to water soluble organics (WSO) followed by their deoxygenation to bio-oil whose yield depend on the catalyst, process gas and process parameters.

HTL of sugarcane bagasse was studied at 280 °C and 7 MPa for 15 min in the presence of K_2CO_3 and KOH homogeneous catalysts and found an increase in conversion by 11 and 17% while an increase in bio-oil yield by 15 and 13% respectively compared to non-catalytic HTL [15]. Solid alkali catalysts, $MgMO_x$, (where: M = Mn, Ni, Fe, Cr, Zn, and Al), were studied for the HTL of sugarcane bagasse and got higher conversion but lower bio-oil yield compared to non-catalytic run [16]. In another study of catalytic HTL of sugarcane bagasse, homogeneous NaOH catalyst reportedly gave higher conversion but lower bio-oil yield compared to heterogeneous ZSM-5 catalyst [17]. Higher conversion observed in the presence of NaOH was attributed to its ability to catalyze the depolymerisation of lignocellulose of bagasse to WSO by hydrolysis, being a strong base, but was not able to deoxygenate the WSO to bio-oil. Whereas the higher bio-oil yield obtained over ZSM-5 was owing to its higher catalytic activity to deoxygenate the WSO to bio-oil, since the depolymerisation of lignocellulose of bagasse to WSO was catalyzed by H^+ and OH^- furnished by hot compressed water itself [11]. Thus the heterogeneous catalysts have the advantage of higher bio-oil yield besides being recovered and reused and heterogeneous catalysts studied for the HTL of lignocellulose biomass were reviewed [18].

Our earlier study reported the effect of Fe-MCM-41 synthesized with the crystallization time of 24 h on the HTL of sugarcane bagasse along with 11 other catalysts under fixed reaction conditions, using both CO and H_2 as process gas [19]. %Conversion, %bio-oil yield and %oxygen in bio-oil were found to be 75.6, 51.1, and 32.3%, respectively in the presence of H_2, while 83.6, 56.2, and 17.7%, respectively in the presence of CO, thus CO was concluded to be the better process gas. The present study is aimed at expanding the scope further by synthesizing Fe-MCM-41 with varying crystallization time, characterize and evaluate for the HTL of sugarcane bagasse under the same fixed process conditions to correlate them. Further to identify the Fe-MCM-41 catalyst that gives the highest yield of bio-oil containing the least oxygen content and to study the effect of process parameters on its catalytic performance.

2. Materials and Methods

2.1 Materials

Sodium metasilicate (Aldrich), ferric nitrate monohydrate (Hi Media), N-Cetyl-N,N,N trimethyl ammonium bromide (Loba) and sulphuric acid AR (Rankem) were used for the synthesis of Fe-MCM-41 catalysts. Diethyl ether, ethyl acetate and acetone used in the product separation were AR grade of Rankem make. Sugarcane bagasse was kindly provided by Doiwala Sugar Company Limited, Doiwala, Uttarakhand, India and the same was milled, screened to get particles of diameter less than 0.30 mm, dried for 24 h at 115 °C in an air oven, stored in a desiccator at room temperature and used for HTL studies. Carbon monoxide of UHP grade used as process gas in the HTL was supplied by Gupta Industrial Gases.

2.2 Synthesis and Characterization of Fe-MCM -41

An amount of 50 mL of distilled water was taken into a polypropylene bottle to which 28.42 g of sodium metasilicate was added and stirred for 30 min. To this, ferric nitrate solution (0.202 g dissolved in 10 mL of distilled water) was added drop wise under stirring and aged for 1 h. Then H_2SO_4 (80 mL, 2 N) was added drop wise, resulted in pH of 10. Again the mixture was aged for 2 h under stirring resulted in a gel to which N-cetyl-N,N,N-trimethyl ammonium bromide solution (6.728 g dissolved 20 mL of distilled water) was added dropwise and stirred for another 2 h. The resultant gel of Si/Fe atomic ratio of 200 was transferred into a Teflon-lined stainless steel autoclave, closed, and kept in the hot air oven maintained at 150 °C. After the desired crystallization time viz. 12, 18, 24, 36, 48, 60, and 72 h, the autoclave was removed from the air oven and cooled in a running water stream. The contents were filtered and the filter cake was washed with distilled water till the pH of the washings became 10. The washed filter cake was dried at 110 °C for 4 h in a hot air oven and then calcined at 550 °C for 6 h in an electrical muffle furnace. The catalyst samples thus obtained with different crystallization time were labelled as Fe-MCM-41 (X), where 'X' is the crystallization time in h.

Powder X-ray diffraction (XRD) pattern of all the calcined samples were recorded in the 2θ range of 1–10° with Bruker D8 Advance diffractometer, using nickel-filtered Cu-Kα radiation (λ = 1.54 Å), and liquid nitrogen cooled germanium solid-state detector. Unit cell parameter was calculated by indexing the reflection line at 2θ of 2.28° corresponding to (100) plane on a hexagonal unit cell. The BET surface area, BJH pore volume, and pore size distribution were determined from the nitrogen adsorption measurements carried out at −195.85 °C using Micromeritics ASAP-2020 with the built-in software. Prior to the nitrogen adsorption, samples were degassed for 8 h at 200 °C and 1.3×10^{-3} Pa. Wall thickness, a measure of orderliness of the hexagonal structure of MCM-41 was calculated by subtracting pore diameter from unit cell parameter [20]. The Scanning Electron Microscope (SEM) images and Energy Dispersive X-ray (EDX) analysis were recorded using SEM- Zeiss EVO-40 EP with 30nm (HV SE) resolution.

2.3 HTL of Sugarcane Bagasse

2.3.1 Effect of crystallization time of Fe-MCM-41 on the HTL of sugarcane bagasse

High pressure stainless steel batch reactor of 170 mL with a magnetic stirrer (BR 100 Berghof) was used for studying the HTL of sugarcane bagasse, and the schematic diagram of the reactor assembly was described elsewhere [19]. For each catalytic HTL run, 70 mL of distilled water was taken in to the reactor to which 1 g of catalyst was added, followed by the addition of 2.5 g of sugarcane bagasse under stirring. After closing the reactor, it was purged with CO and then filled with the same, till the initial pressure reached 45 bar. The gas inlet was closed and the reactor was heated to 250 °C at the rate of 20 °C/min, and maintained for 120 min under magnetic stirring. Then the reactor was cooled to room temperature, the gaseous products were passed through the CO incinerator, and vented into atmosphere. The remaining product mixture was separated into Oil 1 (ether extract of liquid product), Oil 2 (ethyl acetate extract of liquid product), WSO, Oil 3 (acetone extract of solid product) and Solid Residue (SR) by following the reported procedure [19]. While for non-catalytic HTL run, the same procedure was followed, except the addition of 1 g of catalyst. %Yield of the products, %Yield of total oil and %Oxygen in total oil were calculated using the equations reported thereof. Best catalyst was identified on the basis of the highest %Yield of total oil and the lowest %Oxygen in total oil. %Conversion was calculated using the Equation (1).

$$\%Conversion = 100 - \%Solid\ Residue \quad (1)$$

2.3.2 Effect of process parameters on the HTL of sugarcane bagasse

For the best catalyst identified, effect of various process parameters on its performance for the HTL of sugarcane bagasse was studied by varying one process parameter at a time. Reaction time, catalyst/biomass weight ratio and water/biomass weight ratio were varied from 0 to 120 min, 0 to 0.6 and 15 to 40, respectively. For the effect of reaction time of 0 min, the reactor after reaching the reaction temperature of 250 °C (took 10 min time from switching on), was immediately switched off and the rest of the procedure was same as described before. Similarly the effect of other process parameters namely catalyst/biomass weight ratio and

water/biomass weight ratio were studied by varying them while keeping the all other process parameters as in the previous section. Duplicate runs were carried out for each experiment and the results reported were average of them and the maximum deviation between the results of the duplicate runs were within 3%.

3. Results and Discussion

3.1 Characterization of Fe-MCM-41

From the XRD pattern of the Fe-MCM-41 samples obtained at different crystallization time (Figure 1), it was found that the samples obtained after 12 and 18 h of crystallization time did not show any peaks. The sample obtained after 24 h of crystallization time showed all the three reported characteristic peaks of Fe-MCM-41, a predominant peak at 2θ of 2.28° and two higher order peaks at 3.91° and 4.49° corresponding to (100), (110), and (200) reflections, respectively [21], indicated the formation of highly ordered hexagonal structure of MCM-41. XRD pattern of the samples synthesized after the crystallization time of 36, and 48 h have shown a very weak peak at 2θ of 2.28° and no higher order peaks, are typically of MCM-50 [22]. XRD pattern of the samples obtained after 60, and 72 h of crystallization time resembled that of triphasic mixture of MCM-41, MCM-50, and amorphous phase [20].

BET surface area, BJH pore volume, pore diameter determined from nitrogen adsorption, unit cell parameter calculated from XRD characterization and Si/Fe ratio calculated from EDX analysis are presented in Table 1. The BET surface area increased with increase in crystallization time from 12 to 24 h, reached the maximum of 1211 m^2/g, and decreased with further increase to 72 h, which was in accordance with the crystallinity of the samples. Wall thickness of Fe-MCM-41(12) and Fe-MCM-41(18) were found to be negative, confirmed their amorphous nature. Wall thickness, and BET surface area of the Fe-MCM-41(24) were similar to the values reported by Szegedi *et al.* [23], thus reaffirmed its highest crystallinity. For the Fe-MCM-41 samples synthesized with crystallization time longer than 24 h, wall thickness deviated from the reported value confirmed the presence of lamellar Fe-MCM-50 and amorphous phases. The Si/Fe ratio of all

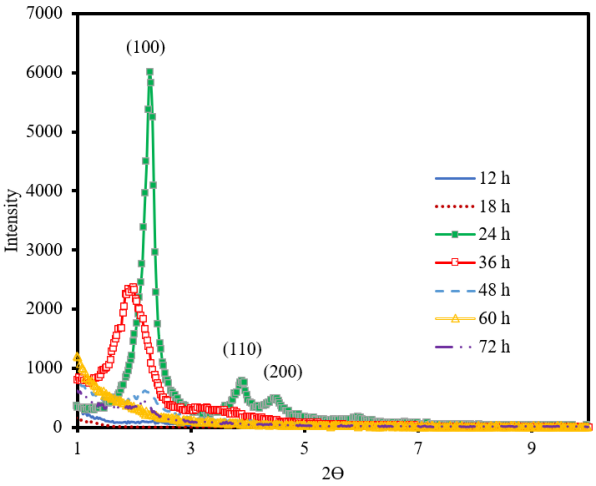

Figure 1. Effect of crystallization time on the crystallinity of Fe-MCM-41.

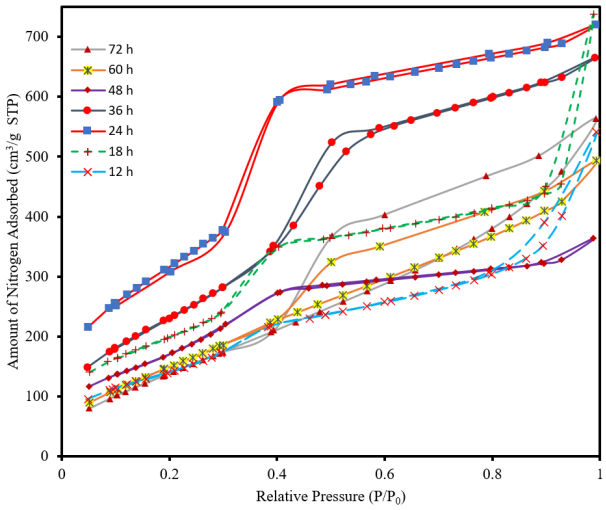

Figure 2. Effect of crystallization time on the adsorption isotherm of Fe-MCM-41.

Table 1. Effect of crystallization time on the physicochemical properties of Fe-MCM-41.

Catalyst Code	Crystallization Time (h)	Si/Fe atomic ratio	BET surface area (m^2/g)	BJH pore volume (cm^3/g)	BJH average pore diameter (nm)	Unit cell parameter (a) (nm)	Wall thickness (nm)
Fe-MCM-41(12)	12	–	542	0.8293	5.7497	4.74	−1.0097
Fe-MCM-41(18)	18	54.8	753	1.182	4.9955	4.5803	−0.4152
Fe-MCM-41(24)	24	81.3	1211	1.1394	3.1071	4.4639	1.3568
Fe-MCM-41(36)	36	79.8	918	1.0247	3.6186	5.2694	1.6508
Fe-MCM-41(48)	48	63.8	686	0.6089	3.0156	4.0781	0.5463
Fe-MCM-41(60)	60	107.1	638	0.7486	4.0406	4.6663	0.6252
Fe-MCM-41(72)	72	94.5	614	0.8712	4.1092	5.0702	0.6793

the Fe-MCM-41 samples synthesized at different crystallization time were found to be less than the Si/Fe ratio of the gel (Si/Fe = 200) from which they were hydrothermally crystallized. This may be due to the preferential transfer of iron from gel to crystalline phase. But no specific trend of variation of Si/Fe atomic ratio of Fe-MCM-41 samples with an increase in crystallization time was observed.

The nitrogen adsorption isotherms of the samples obtained at different crystallization time are presented in Figure 2. Fe-MCM-41(24) and Fe-MCM-41(36) have shown type IV (a) adsorption isotherm with the hysteresis loop H1, characteristic of mesoporous materials. It was comprised of three segments viz. initial monolayer-multilayer adsorption on the walls

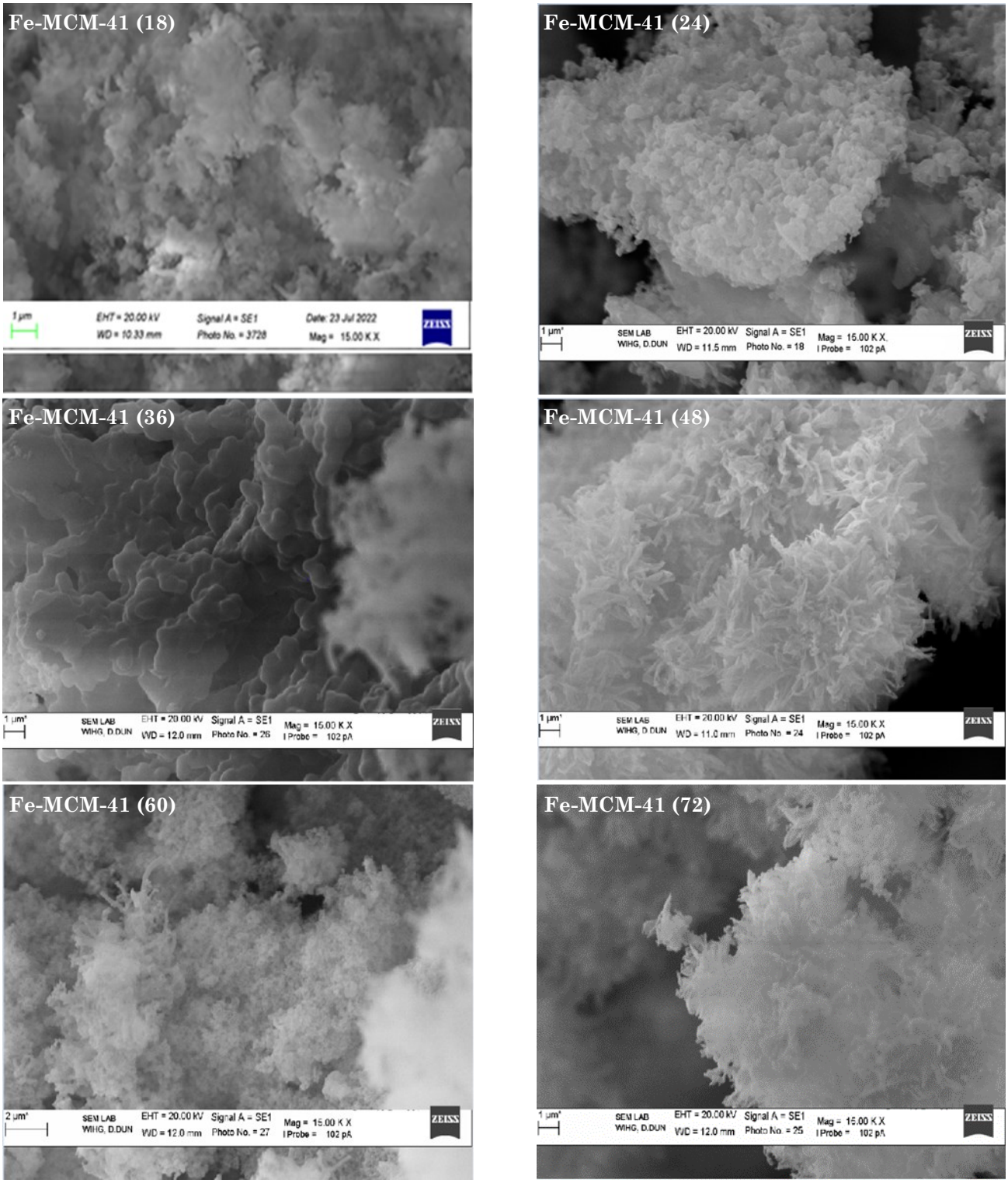

Figure 3. SEM images of Fe-MCM-41 obtained at different crystallization time.

of mesopore, followed by a steep increase in the amount of nitrogen adsorption at P/P^o between 0.3 and 0.4 [20,21] due to mesopore condensation, and a final saturation plateau [24]. The characteristic mesopore condensation at P/P^o between 0.3 and 0.4 was found to be steeper for Fe-MCM-41(24), attributed to its highly ordered hexagonal mesoporous structure, compared to 36 h. The inflection point was not marked with further increase in crystallization time to 48 h, and instead a smooth curve was observed due to the absence of mesopore condensation, indicated that the structure was lamellar MCM-50, a member of M41S-type [25]. Adsorption isotherms of samples obtained after 60 and 72 h were of type II with hysteresis loop of H3, characteristic of loose aggregates of plate-like particles [26,27].

The SEM images of the Fe-MCM-41 samples obtained after different crystallization time viz. 24, 36, 48, 60, and 72 h are presented in Figure 3. The SEM morphology of the sample Fe-MCM-41(24) was similar to the reported [21] image of Fe-MCM-41. A distinct morphology of part of the sample Fe-MCM-41(36), different from the rest may be of MCM-50, indicated the beginning of transformation of MCM-41 to MCM-50, thus reaffirmed the XRD result. This transformation became complete in 48 h, as inferred from its sandy rose like morphology, reportedly [20] that of MCM-50. The morphology of Fe-MCM-41(60) and Fe-MCM-41(72) were similar but distinct from the rest of the samples, which may be of the triphasic mixture of MCM-41, MCM-50, and amorphous phase [20].

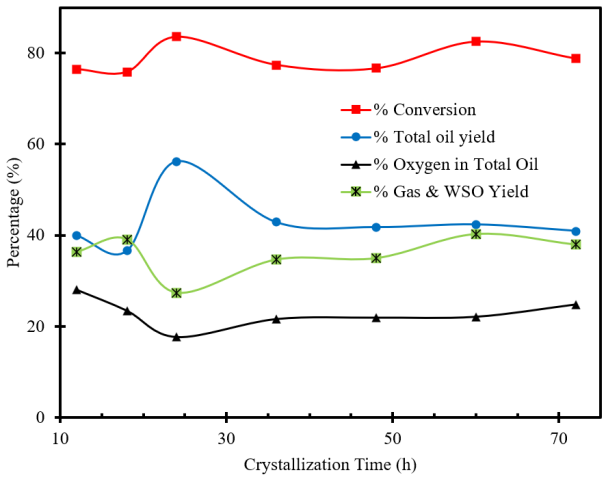

Figure 4. Effect of crystallization time of Fe-MCM-41 on the catalytic performance of HTL of sugarcane bagasse. (Reaction time: 120 min, Temperature: 250 °C, Initial CO pressure: 45 bar, Catalyst/Biomass weight ratio: 0.4, Water/Biomass weight ratio: 28).

From these characteristics, it may be concluded that the crystallization of hexagonal Fe-MCM-41 occurred after 24 h, its transformation to lamellar Fe-MCM-50 took place between 36 to 48 h, after which their amorphisation began. Further, the kinetics of Fe-MCM-41 observed in the present study was similar to MCM-41, may be because both the studies used N-cetyl-N,N,N-trimethyl ammonium bromide as the organic structure directing agent [20].

3.2 Effect of Crystallization Time of Fe-MCM-41 on the HTL of Sugarcane Bagasse

Effect of crystallization time of Fe-MCM-41 on the catalytic performance of HTL of sugarcane bagasse is presented in Figure 4. The highest %Conversion was found to be 83.6% over Fe-MCM-41(24) catalyst whereas for all other Fe-MCM-41 catalysts, conversion was found to be less than the non-catalytic HTL conversion of 83%. Conversion of sugarcane bagasse by the hydrolysis of its lignocellulose was mainly catalysed by H^+ and OH^- furnished by subcritical water [11]. Presence of amorphous and lamellar MCM-50 phases in Fe-MCM-41 catalysts other than Fe-MCM-41(24) as inferred from XRD characterization, might have catalyzed the re-polymerization of bio-oil components into char whose separate quantification was not possible, since it was present together with the unconverted sugarcane bagasse, as SR. On the other hand, all the Fe-MCM-41 catalysts gave higher %Total oil yield, lower %Gas & WSO yield, and %Oxygen in total oil compared to non-catalytic HTL, confirming their deoxygenation activity in converting the WSO to low oxygen containing bio-oil. Among all the Fe-MCM-41 catalysts studied, the best catalyst was found to be Fe-MCM-41(24) as it gave the highest %Total oil yield of 56.2, the lowest %Gas & WSO yield of 27.4, and the lowest %Oxygen in total oil of 17.7, attributed to its highest crystallinity and surface area. Under the same process conditions of HTL of sugarcane bagasse, simple iron oxide catalyst with BET surface area of 307.1 m^2/g was reported to give %Total oil yield, %Gas & WSO yield, and %Oxygen in total oil of 49.2, 32.8, and 19.7%, respectively [19]. Thus the higher deoxygenation activity shown by Fe-MCM-41(24) may be also because of thorough dispersion of iron on a silica framework of MCM-41, containing mesoporous channels allowed its access to WSO, unlike simple iron oxide catalyst.

3.3 Effect of Process Parameters on the Catalytic Activity of Fe-MCM-41(24) for the HTL of Sugarcane Bagasse

3.3.1 Effect of reaction time

Effect of reaction time on the HTL of sugarcane bagasse over Fe-MCM-41(24) is presented in Figure 5. Conversion of 64.5% observed at 0 min was mainly due to the hydrolysis of cellulose and hemicellulose together constituted 70-80% of sugarcane bagasse [8], as they were reportedly hydrolyzed completely in 2 min at 280 °C [28], and 230 °C [29], respectively. With an increase in reaction time from 0 to 15 min, both %Conversion and %Gas & WSO yield increased by 5% due to the hydrolysis of lignocellulose of sugarcane bagasse to water soluble sugars and phenols, while %Total oil yield remained almost the same. From 15 to 30 min, %Total oil yield increased by 13% accompanied by a similar decrease in the %Gas & WSO yield, while %Conversion almost remained the same. From these observations, it may be concluded that the conversion of lignocellulose of sugarcane bagasse to WSO by hydrolysis and deoxygenation of WSO to bio-oil occurred consecutively, similar to the findings reported over iron-cobalt oxide catalyst [30]. Doubling of reaction time from 30 to 60 min did not result in any significant change, whereas further doubling to 120 min, increased the %Total oil yield by 20.7 due to both an increase in the %Conversion by 12.9%, possibly of the lignin part, reportedly slow in getting hydrolyzed [31] and a decrease in the %Gas & WSO yield by 7.8%. Interestingly, %Oxygen in total oil decreased only by 2.4% from 60 to 120 min and for the entire increase in reaction time from 0 to 120 min, the same decreased from 21.4 to 17.7% only. This is in contrast to a decrease from 26.6 to 20.4% from 15 to 60 min and a sharp decrease to 10.8% from 60 to 120 min reported over iron-cobalt oxide catalyst [30]. Thus it may be concluded that deoxygenation of bio-oil to low oxygen containing oil, a distinct consecutive step reported for iron-cobalt oxide catalyst is absent in the present Fe-MCM-41 catalyst. This may be possibly the cobalt in iron-cobalt oxide catalyst be responsible for the subsequent deoxygenation of bio-oil to low oxygen containing bio-oil and hence the catalytic activity of Fe-Co-MCM-41 on the HTL of sugarcane bagasse is worth investigating in the future.

3.3.2 Effect of Catalyst/Biomass (C/B) weight ratio

%Conversion of sugarcane bagasse did not show any specific trend of variation with an increase in the C/B ratio (Figure 6) as the same was catalyzed by the hot compressed water and independent of the Fe-MCM-41 catalyst. %Total oil yield increased marginally from 35.22 to 35.4 whereas %Oxygen in total oil decreased from 31.5 to the lowest of 15.3% with an increase in C/B ratio from 0 to 0.2, indicated its strong deoxygenation activity in converting bio-oil to low oxygen containing bio-oil. Further increase in C/B ratio to 0.4 significantly increased the %Total oil yield to the highest of

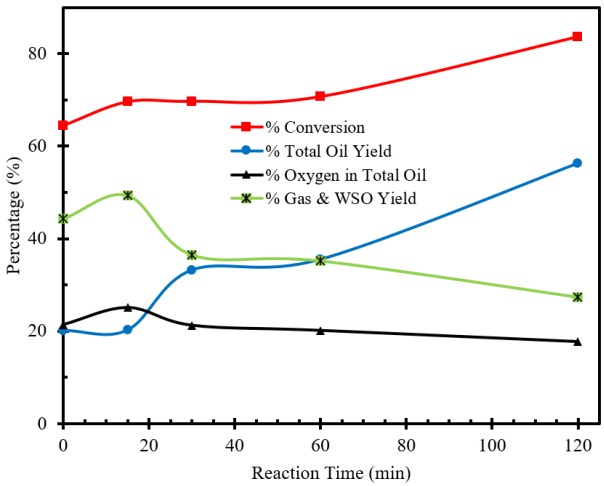

Figure 5. Effect of reaction time on the catalytic performance of HTL of sugarcane bagasse. (Catalyst: Fe-MCM-41 (24), Temperature: 250 °C, Initial CO pressure: 45 bar, Catalyst / Biomass weight ratio: 0.4, Water/Biomass weight ratio: 28).

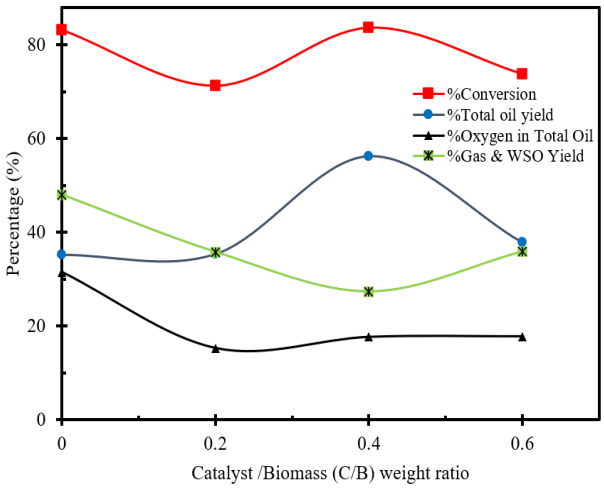

Figure 6. Effect of Catalyst/biomass (C/B) weight ratio on the catalytic performance of HTL of sugarcane bagasse. (Catalyst: Fe-MCM-41 (24), Reaction time: 120 min, Temperature: 250 °C, Initial CO pressure: 45 bar, Water / Biomass weight ratio: 28).

56.2% and hence marginally increased the %Oxygen in total oil to 17.7%. Subsequent increase in C/B ratio to 0.6, drastically decreased the %Total oil yield to 37.8% though the %Oxygen in total oil only marginally increased to 17.8%. This may be because of the repolymerization of bio-oil components to solid residue which would have masked the active centers responsible for the deoxygenation of WSO to bio-oil. Similar trend was observed for the HTL of sugarcane bagasse under the identical process conditions over iron-cobalt oxide catalyst (Co/Fe atomic ratio of 1.09), but both the maximum %Total oil yield of 57.6 and the minimum %Oxygen in total oil of 10.8 were obtained at the same C/B ratio 0.4 [30].

3.3.3 Effect of Water/Biomass (W/B) weight ratio

With an increase in the W/B ratio from 15 to 28, %Total oil yield increased by 16.9 due to both an increase in %Conversion and a decrease in %Gas & WSO yield by 9.9 and 7%, nrespectively (Figure 7). This may be because, increase in water increased the first step of hydrolysis of lignocellulose to WSO, hence higher deoxygenation of WSO to bio-oil. Further increase in W/B ratio from 28 to 40, decreased the %Total oil yield by 19.1 due to both decrease in %Conversion and increase in %Gas & WSO yield by 9.3 and 9.8, respectively. This may be possibly because the WSO was solvated and stabilized by the large excess of water, thereby retarding its deoxygenation to bio-oil which in turn suppresses the preceding step of hydrolysis of lignocellulose to WSO, clearly reaffirms that these two consecutive reactions are equilibrium controlled. With an increase in W/B ratio from 15 to 40, %Oxygen in total oil increased continuously from 12.3 to 20.4 which is contrary to the trend of initial decrease followed by an increase reported over iron-oxide catalyst [30].

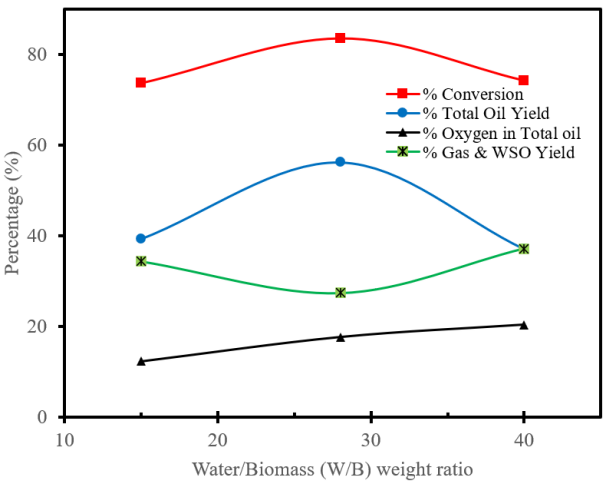

Figure 7. Effect of Water/Biomass (W/B) weight ratio on the catalytic performance of HTL of sugarcane bagasse. (Catalyst: Fe-MCM-41 (24), Reaction time: 120 min, Temperature: 250 °C, Initial CO pressure: 45 bar, Catalyst/Biomass weight ratio: 0.4).

4. Conclusion

Increase in crystallization time from 12 to 24 h increased the crystallinity of Fe-MCM-41, further increase to 48 h, transformed Fe-MCM-41 to Fe-MCM-50, and beyond which amorphisation occurred. All the Fe-MCM-41 catalysts gave higher oil yield with lower oxygen content compared to non-catalytic HTL, confirmed their deoxygenation activity. Among them, Fe-MCM-41 obtained after the crystallization time of 24 h gave the highest bio-oil yield of 56.2% with the least oxygen content of 17.7% owing to its highest crystallinity leading to thorough dispersion of iron on a hexagonal mesoporous silica framework of MCM-41. Overall HTL of sugarcane bagasse was found to be comprised of two consecutive equilibrium, first the hydrolysis of lignocellulose to WSO and second the deoxygenation of WSO to bio-oil. The highest bio-oil yield and the least oxygen content were obtained with the reaction time of 120 min, 250 °C, initial CO pressure of 45 bar, Water/Biomass weight ratio of 28 and Catalyst/Biomass weight ratio of 0.4 and 0.2, respectively.

Acknowledgement

The authors great fully thank the Ministry of New and Renewable Energy, Government of India for the financial support (Grant number F.No.7/184/2013-B F).

References

[1] Nel, W.P., Cooper, C.J. (2009). Implications of fossil fuel constraints on economic growth and global warming. *Energy Policy*, 37(1), 166–180. DOI: 10.1016/j.enpol.2008.08.013.

[2] Iyer, G.C., Edmonds, J.A., Fawcett, A.A., Hultman, N.E., Alsalam, J., Asrar, G.R., Calvin, K. V., Clarke, L.E., Creason, J., Jeong, M., Kyle, P., McFarland, J., Mundra, A., Patel, P., Shi, W., McJeon, H.C. (2015). The contribution of Paris to limit global warming to 2 °c. *Environmental Research Letters*, 10(12) 125002. DOI: 10.1088/1748-9326/10/12/125002.

[3] Jeswani, H.K., Figueroa-Torres, G., Azapagic, A. (2021). The extent of food waste generation in the UK and its environmental impacts. *Sustainable Production and Consumption*, 26, 532–547. DOI: 10.1016/j.spc.2020.12.021.

[4] Fulton, L.M., Lynd, L.R., Körner, A., Greene, N., Tonachel, L.R. (2015). The need for biofuels as part of a low carbon energy future. *Biofuels, Bioproducts and Biorefining*, 9(5), 476–483. DOI: https://doi.org/10.1002/bbb.1559.

[5] Chandel, A.K., Garlapati, V.K., Jeevan Kumar, S.P., Hans, M., Singh, A.K., Kumar, S. (2020). The role of renewable chemicals and biofuels in building a bioeconomy. *Biofuels, Bioproducts and Biorefining*, 14(4), 830–844. DOI: 10.1002/bbb.2104.

[6] Lynd, L.R., Liang, X., Biddy, M.J., Allee, A., Cai, H., Foust, T., Himmel, M.E., Laser, M.S., Wang, M., Wyman, C.E. (2017). Cellulosic ethanol: status and innovation. *Current Opinion in Biotechnology*, 45, 202–211. DOI: 10.1016/j.copbio.2017.03.008.

[7] Zhou, C.H., Xia, X., Lin, C.X., Tong, D.S., Beltramini, J. (2011). Catalytic conversion of lignocellulosic biomass to fine chemicals and fuels. *Chemical Society Reviews*, 40(11), 5588–5617. DOI: 10.1039/c1cs15124j.

[8] Bezerra, T.L., Ragauskas, A.J. (2016). A review of sugarcane bagasse for second-generation bioethanol and biopower production. *Biofuels, Bioproducts and Biorefining*, 10(5), 634–647. DOI: https://doi.org/10.1002/bbb.1662.

[9] Gopal, A.R., Kammen, D.M. (2009). Molasses for ethanol: The economic and environmental impacts of a new pathway for the lifecycle greenhouse gas analysis of sugarcane ethanol. *Environmental Research Letters*, 4(4), 044005. DOI: 10.1088/1748-9326/4/4/044005.

[10] Nunes, L.J.R., Loureiro, L.M.E.F., Sá, L.C.R., Silva, H.F.C. (2020). Sugarcane industry waste recovery: A case study using thermochemical conversion technologies to increase sustainability. *Applied Sciences (Switzerland)*, 10(18), 6481. DOI: 10.3390/APP10186481.

[11] Toor, S.S., Rosendahl, L., Rudolf, A. (2011). Hydrothermal liquefaction of biomass: A review of subcritical water technologies. *Energy*, 36(5), 2328–2342. DOI: 10.1016/j.energy.2011.03.013.

[12] Ariyawansha, T., Abeyrathna, D., Ahamed, T., Noguchi, R. (2020). Integrated bagasse utilization system based on hydrothermal liquefaction in sugarcane mills: theoretical approach compared with present practices. *Biomass Conversion and Biorefinery*, 12, 27–37. DOI: 10.1007/s13399-020-00958-w.

[13] Ramirez, J.A., Rainey, T.J. (2019). Comparative techno-economic analysis of biofuel production through gasification, thermal liquefaction and pyrolysis of sugarcane bagasse. *Journal of Cleaner Production*, 229, 513–527. DOI: 10.1016/j.jclepro.2019.05.017.

[14] Gollakota, A.R.K., Kishore, N., Gu, S. (2018). A review on hydrothermal liquefaction of biomass. *Renewable and Sustainable Energy Reviews*, 81, 1378–1392. DOI: 10.1016/j.rser.2017.05.178.

[15] Singh, R., Prakash, A., Balagurumurthy, B., Singh, R., Saran, S., Bhaskar, T. (2015). Hydrothermal liquefaction of agricultural and forest biomass residue: comparative study. *Journal of Material Cycles and Waste Management*, 17(3), 442–452. DOI: 10.1007/s10163-014-0277-3.

[16] Long, J., Li, Y., Zhang, X., Tang, L., Song, C., Wang, F. (2016). Comparative investigation on hydrothermal and alkali catalytic liquefaction of bagasse: Process efficiency and product properties. *Fuel*, 186, 685–693. DOI: 10.1016/j.fuel.2016.09.016.

[17] Yan, X., Ma, J., Wang, W., Zhao, Y., Zhou, J. (2018). The effect of different catalysts and process parameters on the chemical content of bio-oils from hydrothermal liquefaction of sugarcane bagasse. *BioResources*, 13(1), 997–1018. DOI: 10.15376/biores.13.1.997-1018.

[18] Scarsella, M., de Caprariis, B., Damizia, M., De Filippis, P. (2020). Heterogeneous catalysts for hydrothermal liquefaction of lignocellulosic biomass: A review. *Biomass and Bioenergy*, 140, 105662. DOI: 10.1016/j.biombioe.2020.105662.

[19] Govindasamy, G., Sharma, R., Subramanian, S. (2019). Studies on the effect of heterogeneous catalysts on the hydrothermal liquefaction of sugarcane bagasse to low-oxygen-containing bio-oil. *Biofuels*, 10(5), 665–675. DOI: 10.1080/17597269.2018.1433967.

[20] Blin, J.L., Otjacques, C., Herrier, G., Su, B.L. (2001). Kinetic study of MCM-41 synthesis. *International Journal of Inorganic Materials*, 3(1), 75–86. DOI: 10.1016/S1466-6049(00)00043-X.

[21] Atchudan, R., Pandurangan, A., Somanathan, T. (2009). Bimetallic mesoporous materials for high yield synthesis of carbon nanotubes by chemical vapour deposition techniques. *Journal of Molecular Catalysis A: Chemical*, 309(1–2), 146–152. DOI: 10.1016/j.molcata.2009.05.010.

[22] Huo, Q., Margolese, D.I., Stucky, G.D. (1996). Surfactant Control of Phases in the Synthesis of Mesoporous Silica-Based Materials. *Chemistry of Materials*, 8(5), 1147–1160. DOI: 10.1021/cm960137h.

[23] Szegedi, Á., Kónya, Z., Méhn, D. óra, Solymár, E., Pál-Borbély, G., Horváth, Z.E., Biró, L.P., Kiricsi, I. (2004). Spherical mesoporous MCM-41 materials containing transition metals: Synthesis and characterization. *Applied Catalysis A: General*, 272(1–2), 257–266. DOI: 10.1016/j.apcata.2004.05.057.

[24] Thommes, M., Kaneko, K., Neimark, A. V., Olivier, J.P., Rodriguez-Reinoso, F., Rouquerol, J., Sing, K.S.W. (2015). Physisorption of gases, with special reference to the evaluation of surface area and pore size distribution (IUPAC Technical Report). *Pure and Applied Chemistry*, 87(9–10), 1051–1069. DOI: 10.1515/pac-2014-1117.

[25] Kresge, C.T., Roth, W.J. (2013). The discovery of mesoporous molecular sieves from the twenty year perspective. *Chemical Society Reviews*, 42(9), 3663–3670. DOI: 10.1039/c3cs60016e.

[26] Sing, K.S.W., Williams, R.T. (2004). Physisorption hysteresis loops and the characterization of nanoporous materials. *Adsorption Science and Technology*, 22(10), 773–782. DOI: 10.1260/0263617053499032.

[27] Cychosz, K.A., Guillet-Nicolas, R., García-Martínez, J., Thommes, M. (2017). Recent advances in the textural characterization of hierarchically structured nanoporous materials. *Chemical Society Reviews*, 46(2), 389–414. DOI: 10.1039/c6cs00391e.

[28] Rogalinski, T., Liu, K., Albrecht, T., Brunner, G. (2008). Hydrolysis kinetics of biopolymers in subcritical water. *Journal of Supercritical Fluids*, 46(3), 335–341. DOI: 10.1016/j.supflu.2007.09.037.

[29] Mok, W.S.L., Antal, M.J. (1992). Uncatalyzed Solvolysis of Whole Biomass Hemicellulose by Hot Compressed Liquid Water. *Industrial and Engineering Chemistry Research*, 31(4), 1157–1161. DOI: 10.1021/ie00004a026.

[30] Govindasamy, G., Sharma, R., Subramanian, S. (2020). Effect of composition of iron-cobalt oxide catalyst and process parameters on the hydrothermal liquefaction of sugarcane bagasse. *Bulletin of Chemical Reaction Engineering & Catalysis*, 15(1), 186–198. DOI: 10.9767/bcrec.15.1.5385.186-198.

[31] Karagöz, S., Bhaskar, T., Muto, A., Sakata, Y. (2005). Comparative studies of oil compositions produced from sawdust, rice husk, lignin and cellulose by hydrothermal treatment. *Fuel*, 84(7–8), 875–884. DOI: 10.1016/j.fuel.2005.01.004.